A MODELING AND SIMULATION PLATFORM FOR SPACE-BASED COMPARTMENTAL MODELING OF PANDEMIC SPREAD

Román Cárdenas

Laboratorio de Sistemas Integrados
Universidad Politécnica de Madrid
ETSI Telecomunicación, Avenida Complutense 30
Madrid 28040, SPAIN
r.cardenas@upm.es

Alonso Inostrosa-Psijas

Escuela de Ingeniería Informática
Universidad de Valparaíso
General Cruz 222
Valparaíso, CHILE
alonso.inostrosa@uv.cl

Gabriel Wainer

Dept. Of Systems and Computer Engineering
Carleton University
1125 Colonel By Drive
Ottawa ON K1S 5B6, CANADA
gwainer@sce.carleton.ca

ABSTRACT

The COVID-19 outbreak has shown that Modeling and Simulation (M&S) methodologies are an important aspect to study the spread of the disease and assess the effect of different measures to diminish its negative effect. Although traditional models have been widely used, there is a need to build new, highly configurable disease models to explore multiple scenarios quickly. We present an M&S framework to perform rapid prototyping of pandemic spread using the Cell-DEVS space-based discrete-event modeling approach. This method supports age segmentation of the population, hospital-capacity-dependent deaths, and enforcing mobility restriction policies. This method is useful for studying the spread of the disease, as well as combining the simulation results with different visualization tools.

Keywords: cellular models, Cell-DEVS, compartmental models, pandemics, SIRDS model.

1   INTRODUCTION

SARS-CoV-2 (COVID-19) is a highly contagious viral disease that spread worldwide in less than four months. As of March 19th, 2021, there have been more than 121 million cases globally and over 2.6 million deaths caused by the virus (Du et al. 2020). Authorities in each country have taken different measures to control contagions, some more successfully than others. In this aspect, mathematical models and computer simulations may help officials in the development of health strategies to tackle the expansion of the disease. Simulation models that can describe the dynamics of contagious diseases and predict the time course and behavior of contagions spread in a population are a key tool that can be used as a testbed for trying different health policies to control pandemics (Muscatello, et al. 2017).

Current studies of COVID-19 use a variety of methods to study the dynamics of the disease (Danon, et al. 2020, Caccavo 2020). These studies are mainly based on i) Agent-Based Simulations, ii) Analytical models (mainly through Ordinary Differential Equations (ODEs)) and iii) Cellular Automata (CA). Here, we discuss a method to define complex models of the spread of diseases using a space-based approach (Cárdenas et al 2020) that can include the benefits of these three approaches. The method also makes it easy to add new disease model parameters. Similarly, combining the results with visualization tools and advanced graphical interfaces (including Jupyter notebooks, Geographical Information Systems (GISs), Building Information Models (BIMs), and spatial diagrams) is straightforward.

The method is based on Cell-DEVS (Wainer 2009), which divides the space under study into a grid through the discretization of the original equations. The notation makes it easy to encode within a computer program. Adding new aspects to the models is easily accomplished, as is providing mechanisms to combine the models with the built environment (buildings, cities, transportation).

In the following sections, we discuss the methodology, the tools to build epidemiological models, how to add new experimental results, new parameters (such as density, gender ratio, age, pre-symptomatic and asymptomatic transmission (Nishiura, et al. 2020)). We discuss different simulation scenarios and analyze the influence of the different parameters, showing the results available on Jupyter notebooks and remote execution servers. This allows us to demonstrate the use of the framework and how researchers can use this method in the modeling process without worrying in implementation details of the platform.

2   RELATED WORK

Most studies of COVID-19 are based on Agent-Based Simulations, ODEs and CA. Agent-based simulation models contagion as an emerging effect of individual agent behavior interaction (Cuevas 2020, Callejas, et al. 2020). This fine-grain modeling sometimes makes it difficult to run large-scale population simulations due to the high computing demands. Most ODE models (Heesterbeek, et al. 2015) are based on models that classify individuals in different "compartments", representing the infection stages of the disease (Kermack and McKendrick 1927). Usually, the weakness of these models is that they assume a homogeneous population (Keeling and Danon 2009) and ignore the variable infection susceptibility of individuals. Similarly, they do not consider the spatial aspects of transmission (Hoya White, et al. 2007).

CA models overcome these shortcomings and model contagious disease spreading (Fuentes and Kuperman 1999, Hoya White, et al. 2007) and, more recently, have also been used to study COVID-19 spreading dynamics in combination with different variations of the compartmental models (Dai, et al. 2021, Ghosh and Bhattacharya 2020, Medrek and Pastuszak 2021).

Our approach combines these three aspects: the individual interactions using a microsimulation approach like those in agent-based models, the spatial features of CA and the advantages of a formal method using mathematical compartmental models (Khalil and Wainer 2020) by combining them using the Cell-DEVS formalism. The following subsections discuss some of the aspects of the related work in these areas.

2.1 Epidemiological SIR Models

Kermack and McKendrick (1927) introduced a model to study the spread dynamics of the Black Death in London. It is one of the most widely used models (Dietz 1967), showing a simple yet effective epidemiological model. Its simplicity relies in dividing the population into compartments related to the stages of the disease through which individuals in a population must pass. Accordingly, population individuals can be Susceptible (S), Infected (I) or Recovered (R). In this SIR model, a person that has never been infected is assigned to the S compartment. Individuals who acquired the disease and can infect others are assigned to the I group. Those who have recovered and are now immune to the disease are assigned to the R compartment. The models contain a set of parameters that affect their dynamics. Different combinations of parameters can lead to scenarios that are catastrophic and others in which the disease subsides naturally (Pacheco and de Lacerda 2021).

SIR models have been extended and adapted, adding more equations representing new compartments or features. SEIR models consider Exposed (E) individuals to incorporate diseases that, upon infection, have an incubation period (Aron and Schwartz 1984). Their dynamics are described by the state diagram in Figure 1. Edges correspond to the functions associated to the change from one stage of the disease to another: Λ is the recruitment rate (i.e., births), β the infection rate, α_1 the morbidity rate, α_2 the recovery rate, ρ the immunity loss rate, μ the mortality rate by other causes than the disease, and δ the mortality rate induced by the disease.
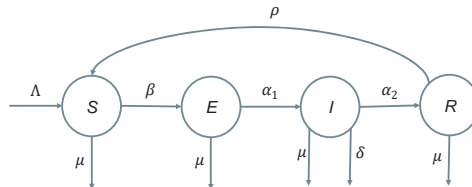

Figure 1. Transition state diagram for the SEIR model.

A system of ODEs can be derived from the diagram, resulting in:

$$\frac{dS}{dt} = \Lambda + \rho R(t) - \beta S(t) - \mu S(t); \quad \frac{dE}{dt} = \beta S(t) - \alpha_1 E(t) - \mu E(t); \quad \frac{dI}{dt} = \alpha_1 E(t) - \alpha_2 I(t) - \mu I(t) - \delta I(t); \quad \frac{dR}{dt} = \alpha_2 I(t) - \rho R(t) - \mu R(t).$$

Other extensions represent vaccination and isolation strategies (Small and Tse 2005). SEIRS models add a new compartment transition in which recovered people lose their immunity after a period (Bjørnstad, et al. 2020). SEIRS models have been successfully used to study spread contagions of malaria (Ngwa and Shu 2000), including models in which a portion of the recovered individuals can infect susceptible (disease-free) mosquitos (Chitnis et al. 2008). Traoré et al. (2017) developed an SEIRS model showing that the transmission of the disease is highly affected by immature anopheles, showing that transmission can be controlled by reducing the population of mosquitos. More recently, SEIRS models have been adapted to the specific parameters of COVID-19. He et al. (2020) developed a model to study COVID propagation in Hubei, China, using a particle swarm optimization algorithm to fit the model's parameters to real data. Rădulescu et al. (2020) analyzed different control strategies in a small town. López and Rodó (2021) also adapted an SEIRS model considering different levels of confinement measures in Italy and Spain, finding that a three-week long drastic lockdown would have strongly reduced contagions.

The SIRDS model (Anderson and May 1992) is another extension that models the spreading of fatal diseases explicitly, by adding a compartment for Deceased (D) individuals. The model includes different features of infection, recovery, and lethality of the disease (Caccavo 2020). Several studies on COVID-19 used this model. Fanelli and Piazza (2020) studied the temporal dynamics of the virus outbreak in China, Italy, and France, and they found that the recovery rate was similar among the different countries. However, infection rate as well as the mortality rate differed. They were able to estimate the number of mechanical ventilation units needed during the peak of the disease. Calafiore et al. (2020) used a variation of the SIRDS model that considers time-varying parameters to capture control measures applied by authorities. The method was applied to the most affected regions of Italy, resulting in accurate predictions for early and late stages over a time window of 41 days. Other SIRD models were used to study the spread progression in India (Chatterjee, et al. 2020) and the USA (Fernández-Villaverde and Jones 2020).

2.2 Cellular Automata Epidemics Modeling

Cellular Automata (CA) are discrete-time models that consist of cells organized as *n*-dimensional infinite lattices. Each of the composing cells has a state (defined by a discrete value) and a local computation function. This local function uses the present value of the cell and a finite set of its neighbor cells to compute the new state. In CA, evolution occurs by means of the parallel execution of each cell's local function at every timestep. These functions, which only depend on the results of a local execution in each cell, generate a global emergent behavior that can be studied at the scale field (Wolfram 2002).

In the context of epidemics, several CA models have used SIR-based approaches to model the spread of contagious diseases (Johansen 1996). Hoya White et al. (2007) proposed a CA implementation of an SIR-like model in which each cell represents a portion of the population, and individuals travel through the cells. Zhong et al. (2009) developed a geographical SIRS CA in which the cell space represents a geographical region with irregular cells of varying dimension. The model was validated for the spreading of SARS in 2003 in the city of Beijing, China. Similarly, López et al (2014) consider an SEIRS-based CA model with probabilistic state transitions. Each cell represents an individual, allowing for individual heterogeneity. Bin et al. (2019) defined an SEIRDS-based CA in which they explore how population density, gender and age can influence the spread of infectious diseases. Each cell represents population density, reducing the computing needs for large populations. The model was tested simulating the spread of Influenza H1N1 in Beijing in 2009, obtaining similar results to real data.

Following the outbreak of the COVID-19 pandemic, several CA models have been proposed. Dai, et al. (2021) proposed a CA model using a SIRD-like approach and reproduced different spread patterns in New York and Iowa. Ghosh and Bhattacharya (2020) added a new compartment to represent infected individuals that require hospitalization or are quarantined. Medrek and Pastuszak (2021) developed an SEIR-based CA for the study of the epidemic trends in Poland, France, and Spain. They included additional parameters, such as age-dependent death rate. The proposed model reproduced mortality rates in accordance with official data for the three countries under study.

Many of the above-mentioned studies consider individuals to be mapped to a cell in a one-to-one fashion, in an agent-based modeling world view. This results in high computing demands for real-world scenarios; therefore, just a fraction of the population is simulated. However, CA are flexible and simple, and they permit the study of spatial population distributions. The discrete-time nature of CA also poses a few shortcomings, as it considers time as isomorphic to natural numbers $\mathbb{N}$ (i.e., time advances at constant steps); thus, cell state changes cannot occur between timesteps (Wainer 2009). Should it occur, the new cell state should either be postponed to the next step or be neglected. This makes it difficult to define advanced timing function conditions for each cell. The Cell-DEVS formalism overcomes these issues by combining CA and the Discrete EVent System Specifications (DEVS) (Zeigler et al. 2000).

2.3 The Cell-DEVS Formalism

Cell-DEVS defines a spatial model as a collection of cells arranged in a grid, using continuous time and discrete-event M&S (Wainer 2009). Cells are DEVS atomic models, and a procedure to couple cells is defined to build a cell space. Figure 2(a) shows a schematic view of a cell: they become active upon the occurrence of external events; otherwise, they remain quiescent. When an input is received, the external transition function triggers a local computation function (t). If the state of the cell changes, an internal transition is scheduled to transmit the new state value after a time specified by the delay function (d).

The local computation function uses values received from its neighborhood (a finite set of nearby cells). The rules are defined by (i) a precondition, (ii) an output value for the cell's state and (iii) a delay time. It means that, if the evaluation of the precondition (i) is satisfied, the cell will change its state and output the new value to its neighborhood (ii) after a delay time (iii). Figure 2(b) shows a cell space where the outputs of a cell are transmitted to the cells in the neighborhood. Cell-DEVS provides a higher level of detail than epidemiological models that consider the population as a whole.
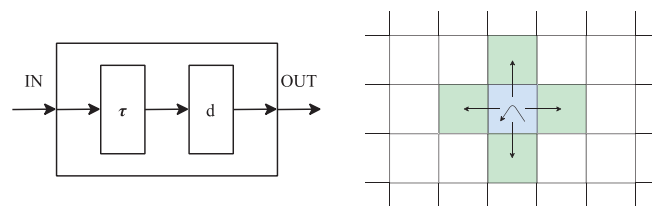

Figure 2. Cell-DEVS model: (a) schematic of a cell; (b) two-dimensional Cell-DEVS model.

3 CELL-DEVS SIRDS COMPARTMENTAL MODEL

We define our Cell-DEVS SIRDS model as an extension of the CA SIR model. Compared to our previous work (Cárdenas et al., 2000), the presented model refines the compartment transition functions, divides the population into age segments, and integrates mobility restriction policies and the effect of congested hospital ICUs. The state of each cell (i, j) at a given time t in the scenario, $\boldsymbol{\theta}_{i,j}^t$, is represented by the 5-tuple:

$$\boldsymbol{\theta}_{i,j}^t = \left\{ \mathbf{P}_{i,j}, \mathbf{S}_{i,j}^t, \mathbf{I}_{i,j}^t, \mathbf{R}_{i,j}^t, \mathbf{D}_{i,j}^t \right\}, \tag{1}$$

where $\mathbf{P}_{i,j}$ corresponds to the population of the region represented by the cell (a fixed parameter), $\mathbf{S}_{i,j}^t$ is the portion of susceptible population, $\mathbf{I}_{i,j}^t$ represents those who are infected, $\mathbf{R}_{i,j}^t$ is the ratio of those who recovered from the disease, and $\mathbf{D}_{i,j}^t$ is the proportion of deceased people. The model divides the population into N age segments (parameters are organized as N-tuples). For example, we refer to the population of cell (i, j) in the nth age segment as $\mathbf{P}_{i,j}[n]$. This allows us to study patterns that depend on the age of the individuals. For each segment, a part of the population becomes infected, as described in Eq (2):

$$\mathbf{i}_{i,j}^t[n] = \mathbf{S}_{i,j}^{t-1}[n] \cdot \mathbf{m}_{i,j}^{t-1,}[n] \cdot \boldsymbol{\sigma}[n] \cdot \mathbf{e}_{i,j}^{t-1}[n] . \tag{2}$$

The ratio of susceptible individuals infected in cell (i, j) at time t depends on the previous susceptible ratio $\mathbf{S}_{i,j}^{t-1}[n]$ multiplied by the *mobility factor* $\mathbf{m}_{i,j}^{t-1,}[n]$ (the probability of an individual in age segment n in cell (i, j) moving to a different area at time $t-1$), the *susceptibility factor* $\boldsymbol{\sigma}[n]$ (the probability of infection of a susceptible individual in age segment n), and the *exposure factor* $\mathbf{e}_{i,j}^{t-1}[n]$ (the probability of exposure of a susceptible individual of age segment n at time $t-1$). For each age segment k of every cell (a, b) in the neighborhood $\mathbf{V}_{i,j}$ of cell (i, j), the exposure factor uses the *connectivity factor* $\mathbf{c}_{i,j}^{a,b}[k]$ (the probability of a person of age k in cell (a, b) moving to cell (i, j)), the population ratio of the age segments involved, the *mobility factor* $\mathbf{m}_{i,j}^{t-1}[k]$ (the probability of an individual of age k in cell (a, b) moving at time $t-1$), and the *virulence factor* $\mathbf{v}[k]$ (i.e., the probability that an infected individual of age k exposes others). The exposure factor cannot be greater than 1. Eq (3) illustrates how to compute $\mathbf{e}_{i,j}^{t-1}[n]$:

$$\mathbf{e}_{i,j}^{t-1}[n] = \min \left\{ 1, \sum_{\substack{a,b \in \mathbf{V}_{i,j} \\ k \in \{1, \cdots, N\}}} \mathbf{c}_{i,j}^{a,b}[k] \cdot \frac{\mathbf{P}_{a,b}[k]}{\mathbf{P}_{i,j}[n]} \cdot \mathbf{I}_{a,b}^{t-1}[k] \cdot \mathbf{m}_{a,b}^{t-1}[k] \cdot \mathbf{v}[k] \right\}. \tag{3}$$

Additionally, $\mathbf{r}_{i,j}^t[n]$ infected individuals recover according to the *recovery factor* $\boldsymbol{\gamma}_{i,j}^{t-1}[n]$, and $\mathbf{d}_{i,j}^t[n]$ individuals die according to the *mortality factor* $\boldsymbol{\varepsilon}_{i,j}^{t-1}[n]$:

$$\begin{aligned} \mathbf{r}_{i,j}^t[n] &= \mathbf{I}_{i,j}^{t-1}[n] \cdot \boldsymbol{\gamma}_{i,j}^{t-1}[n] \\ \mathbf{d}_{i,j}^t[n] &= \mathbf{I}_{i,j}^{t-1}[n] \cdot \boldsymbol{\varepsilon}_{i,j}^{t-1}[n] . \end{aligned} \tag{4}$$

For every cell and age segment, the sum of the recovery and the fatality factors must be less than or equal to 1 at any given time (i.e., $\mathbf{r}_{i,j}^t[n] + \mathbf{d}_{i,j}^t[n]$ cannot be greater than $\mathbf{I}_{i,j}^t[n]$):

$$\boldsymbol{\gamma}_{i,j}^t[n] + \boldsymbol{\varepsilon}_{i,j}^t[n] \leq 1, \forall n \in \{1, \dots, N\} .$$

Finally, depending on the *immunity factor* $\boldsymbol{\omega}[n]$ (the probability of recovered individuals remaining in the recovered compartment), individuals may lose their immunity and become susceptible again:

$$\mathbf{s}_{i,j}^t[n] = \mathbf{R}_{i,j}^{t-1}[n] \cdot (1 - \boldsymbol{\omega}[n]) . \tag{5}$$

Eq. (6) shows how all the compartments are updated for every age segment $n \in \{1, \cdots, N\}$ when the cell's local computation function is triggered:

$$\begin{aligned}
\mathbf{I}_{i,j}^t[n] &= \mathbf{I}_{i,j}^{t-1}[n] + \mathbf{i}_{i,j}^t[n] - \left(\mathbf{r}_{i,j}^t[n] + \mathbf{d}_{i,j}^t[n]\right) \\
\mathbf{R}_{i,j}^t[n] &= \mathbf{R}_{i,j}^{t-1}[n] + \mathbf{r}_{i,j}^t[n] - \mathbf{s}_{i,j}^t[n] \\
\mathbf{D}_{i,j}^t[n] &= \mathbf{D}_{i,j}^{t-1}[n] + \mathbf{d}_{i,j}^t[n] \\
\mathbf{S}_{i,j}^t[n] &= 1 - \left(\mathbf{I}_{i,j}^t[n] + \mathbf{R}_{i,j}^t[n] + \mathbf{D}_{i,j}^t[n]\right).
\end{aligned} \tag{6}$$

3.1 Mobility Restriction Strategies

Kraemer et al. (2020) showed that the COVID-19 outbreak in 2020 was affected by human mobility. Our model allows defining mobility restriction policies in each cell. The value $\mathbf{m}_{i,j}^t$ shown in Eq (8) uses a *base mobility restriction factor* $\mathbf{M}_{i,j}^t[n]$ (mobility restrictions for people of a given age) and a *disobedience factor* $\delta[n]$ (people ignoring the mobility restrictions). We can use age-based restrictions to study reduced mobility of students of different ages, people in long-term care institutions, etc.:

$$\mathbf{m}_{i,j}^t[n] = \delta[n] + (1 - \delta[n]) \cdot \mathbf{M}_{i,j}^t[n]. \tag{8}$$

The value of $\mathbf{M}_{i,j}^t[n]$ depends on the mobility restriction policy applied in cell (i, j) at time t, $\xi_{i,j}^t$. We define four different mobility restriction policies.

Base: There are no restrictions.

Type 1: Cyclic lockdown with scheduled periods of increased economic activity in the whole region (Karin, et al. 2020). There are X different policies $\xi_x, x \in \{0, \cdots X - 1\}$, each of which imposes a mobility restriction factor $\mathbf{M}_x[n]$ that depends on age. The restriction is applied during T_x consecutive days. After this time, the next mobility policy $\xi_{(x+1) \bmod X}$ is applied.

Type 2. Mobility restrictions proportional to the percentage of infected people in each cell. Impact on the mobility $\mathbf{M}[n]$ varies according to age. Mobility is gradually reduced as the total infected ratio grows (9):

$$\mathbf{M}_{i,j}^t[n] = \max\{0, 1 - \mathbf{I}_{i,j}^t \cdot \mathbf{M}[n]\}. \tag{9}$$

Type 3. Mobility restrictions when a threshold of infections is reached, until the ratio decreases. We use X mobility policies $\xi_x, x \in \{0, \cdots X - 1\}$, triggered when the ratio of infected people reaches the *mobility start*, I_x^{start}. Mobility policies are sorted in increasing order of their start trigger (i.e., $I_x^{start} < I_{x+1}^{start} \forall x \in \{0, \cdots X - 1\}$). The policy imposes a mobility restriction $\mathbf{M}_x[n]$ for age segment n until the ratio of infected people reaches the next mobility phase I_{x+1}^{start} or is lower than the *mobility stop*, $I_x^{stop}(I_x^{stop} \leq I_x^{start})$. These triggers provide a hysteresis-like pattern in the mobility restrictions. If at $t - 1$ the mobility policy $\xi_{i,j}^{t-1}$ in cell (i, j) is ξ_x, then $\mathbf{M}_{i,j}^{t-1}[n] = \mathbf{M}_x[n]$. The triggers are applied as follows:

$$\xi_{i,j}^t = \begin{cases} \xi_{x+1} & , \text{if } x < X \text{ and } I_{i,j}^{t-1} \geq I_{x+1}^{start} \\ \xi_{x-1} & , \text{if } x > 1 \text{ and } I_{i,j}^{t-1} < I_x^{stop} \\ \xi_x & , \text{otherwise.} \end{cases} \tag{10}$$

3.2 Modeling Hospital-Capacity-Dependent Deaths

People with severe effects of the disease may need medical assistance. In these cases, hospital capacity may increase mortality for those that cannot receive proper assistance (Wood, et al. 2020). Eq. (11) describes how $\boldsymbol{\gamma}_{i,j}^t[n]$ and $\boldsymbol{\varepsilon}_{i,j}^t[n]$ (recovery and mortality) capture the effect of high hospital capacity in our model:

$$\gamma_{i,j}^t[n] = \begin{cases} \Gamma[n] & \text{, if } I_{i,j}^{t-1} \le I_{i,j}^{cap} \\ \Gamma[n] \cdot (1 - \eta_r[n]) & \text{, otherwise} \end{cases}$$

$$\varepsilon_{i,j}^t[n] = \begin{cases} E[n] & \text{, if } I_{i,j}^{t-1} \le I_{i,j}^{cap} \\ E[n] \cdot (1 + \eta_d[n]) & \text{, otherwise ,} \end{cases} \tag{11}$$

where $\Gamma[n]$ is the *base recovery factor* ($\gamma_{i,j}^t[n]$ if hospital ICUs are not full), $E[n]$ is the *base mortality* ($\varepsilon_{i,j}^t[n]$ if masks are not used), $I_{i,j}^{cap}$ is the *hospital capacity* (minimum ratio of the total infected population to consider that hospital ICUs in the cell are full), and $\eta_r[n]$ and $\eta_d[n]$ the *recovery reduction* and *mortality increment factors* (the impact of congested hospitals on the recovery and the mortality factors, respectively).

4 MODEL IMPLEMENTATION

A Cell-DEVS version of the model presented in Section 3 was implemented using the Cadmium simulator (Belloli, et al. 2019), a C++17 library that can be integrated to other projects easily. Cadmium follows a strong-typed approach to check that all the described models comply with the DEVS formalism at compile time. Additionally, Cadmium supports spatial models based on Cell-DEVS with irregular neighborhoods. To define Cell-DEVS models, we use three auxiliary data structures: one to represent the cell's state; another that contains all the fields used to describe the neighborhood; and one for cell configuration, including additional parameters to modify the model behavior. The implementation in Cadmium is directly derived from the model above. A cell's state is described by the `SIRD` data structure as follows:

```
struct SIRD {
  std::vector<int> population;      // cell population (age-dependent).
  std::vector<double> susceptible;  // ratio of susceptible people (age-dependent).
  std::vector<double> infected;     // ratio of infected people (age-dependent).
  std::vector<double> recovered;    // ratio of recovered people (age-dependent).
  std::vector<double> deceased;     // ratio of deceased people (age-dependent).
  std::vector<double> mobility;     // mobility factor (age-dependent).
}
```

Comparing with Eq. (1), the mobility factor $m_{i,j}^t$ is now part of the state. This allows us to compute the mobility factor and share it with neighboring cells, avoiding duplicate computations. Note that age segment-dependent tuples of the models are implemented using the C++ vector sequence container which dimension is not hard-coded. This allows us to run simulations of models with different numbers of age segments by modifying the model configuration without having to re-compile it. The only element that describes the relationship between neighbors is the connectivity factor $c_{i,j}^{a,b}$ (see Eq. (3)). Thus, the selected neighborhood data structure corresponds to a `std::vector<double>` container.

Cadmium Cell-DEVS models `local_computation` for the local computation function τ and `output_delay` for the output delay function d. When a cell receives an input, the `local_computation` method is triggered. The behavior of `local_computation` is like Eq. (6) plus the calculation of the mobility factor (which is now a part of the cell state). Some of the state values are discretized using the numerical precision defined by the `prec` configuration parameter. The higher precision, the more accurate the results. However, a cell's final state will take longer to converge to a stable value, leading to increased simulation time.

The `output_delay` function defines the time to wait before sending a message with the cell's state change to its neighbors. In this model, `output_delay` is defined as:

```
double output_delay(SIRD const &cell_state) const override { return 1.0 / scaler; }
```

The `scaler` configuration parameter permits the delay applied to all the events to be reduced or increased.

The proposed M&S framework only needs to be compiled once, and it can be used to explore different scenarios by providing a parameter file, enabling the execution of multiple experiments with ease. More

details regarding the implementation of this model and how to configure different simulation scenarios and visualizations can be found in our public GitHub repository.

5   SIRD CELL-DEVS CASE STUDIES

The framework was used to build different scenarios. We used the results in (Hoya White et al. 2007) and (Zhong et al. 2009) to verify the correctness of the results obtained, as the former presents results in accordance with reality for the spreading of infectious diseases and the latter was validated using epidemic data of the SARS outbreak of 2002-2003 of Beijing, China. After building a baseline simulation, the tools can be used to explore how different measures can affect the propagation of a disease.

5.1 Baseline Scenario

The baseline scenario uses a lattice of 25 by 25 cells with 100 individuals per cell. They are divided into four age groups: 20 children, 40 young adults, 20 adults, and 20 elderlies. No mobility restrictions are used. Susceptibility, virulence, and mobility factors correspond to their base values. The remaining parameters of the model can be found in the configuration file of the GitHub repository. Initially, almost the entire population is susceptible to the disease. However, 1% of the young population of the cell (0,0) are infected. Figure 3 shows a simulation output for this case study.
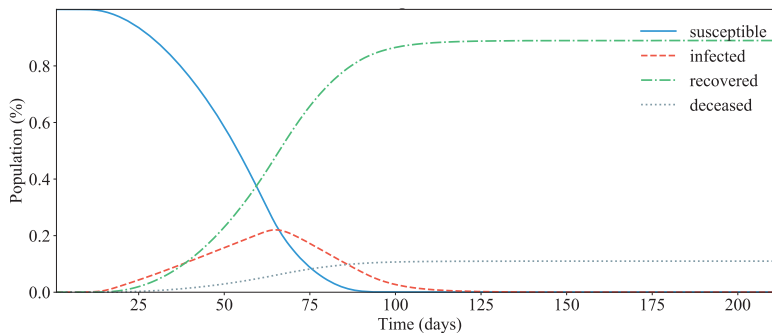

Figure 3. SIRD curves of the baseline scenario.

During the first 10 days, the overall infected ratio is negligible. Then, the number of infected individuals increases until Day 65, which coincides with the infection peak. At the same time, the number of recovered persons increases exponentially. At Day 85, the susceptible ratio is close to 1%. At the end of the simulation, 89% of the population have recovered, whereas 11% of the individuals have died.

5.2 Enforcing Mobility Restrictions

Using our simulation environment, we can execute a variety of experiments with ease. In this way, modelers can explore multiple scenarios to assess the simulated results of different measures. As an illustrative example, we propose three different mobility restriction policies (described in Table 1). Using the same configuration parameters as in the baseline scenario, we explore the effectiveness of these mobility restriction policies, taking into consideration different degrees of disobedience to these restrictions.

Figure 4(a) compares the overall infected ratio peak depending on the applied mobility restriction policy. All the mobility restriction policies can flatten the baseline infection curve, leading to smaller infection ratio peaks and reducing the probability of collapsing hospitals' ICUs. As expected, the higher the percentage of the disobedient population is, the less effective any mobility restriction policy. The *Type 2* mobility restriction policy is less successful when lowering the peak of infections. On the other hand, the *Type 3* policy is the most effective when the disobedience factor is less than 30%. The *Type 1* policy presents more resilience to disobedience and presents better results for disobedience factors over 30%. This is because the mobility restriction factor of this policy is fixed, regardless of the current infection ratio.

Table 1. Configuration parameters of the proposed mobility restriction policies.

Policy Type	Configuration Parameter		Value
Type 1	Phase ξ_0	Mobility restriction, $\mathbf{M}_0$	$\{1, 1, 1, 1\}$
		Phase duration, T_0	4
	Phase ξ_1	Mobility restriction, $\mathbf{M}_1$	$\{0.2, 0.2, 0.2, 0.2\}$
		Phase duration, T_1	3
Type 2	Impact on mobility, $\mathbf{M}$		$\{1, 2, 4, 8\}$
Type 3	Phase ξ_0	Mobility restriction, $\mathbf{M}_0$	$\{1, 1, 1, 1\}$
		Start trigger, I_0^{start}	0
		Stop trigger, I_0^{stop}	0
	Phase ξ_1	Mobility restriction, $\mathbf{M}_1$	$\{0.5, 0.5, 0.5, 0.5\}$
		Start trigger, I_1^{start}	0.05
		Stop trigger, I_1^{stop}	0
	Phase ξ_2	Mobility restriction, $\mathbf{M}_2$	$\{0.2, 0.2, 0.2, 0.2\}$
		Start trigger, I_2^{start}	0.1
		Stop trigger, I_2^{stop}	0.05

Figure 4(b) shows the percentage of the population that remained susceptible during the whole simulation. For disobedience factors below 50%, all the mobility restriction policies can reach herd immunity, and the pandemic is stopped before all the population is infected. However, the *Type 3* restriction policy excels over the other approaches. If all the population obeys the mobility restriction directives, this policy can keep 25% of the population uninfected (15 percentage points higher than the *Type 1* policy). The advantage of *Type 3* policy over the others is significant for disobedience factors below 60%. Scenarios whose disobedience factor is over 60% are not able to reach herd immunity, and end with the susceptible compartment almost empty.
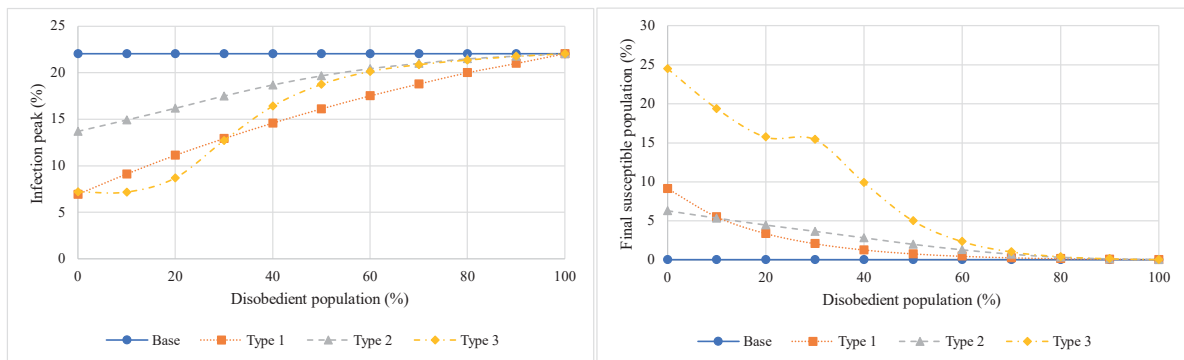

Figure 4. (a) Peak of infections depending on different mobility restriction policies and disobedience factors; (b) Effect of different of lockdown policies on the susceptible compartment.

Figure 5 compares the percentage of deceased people at the end of the simulation depending on the mobility restriction and the disobedience factor. Again, the *Type 3* policy shows the best results, as it can reduce the percentage of deceased people by almost two percentage points compared to the baseline scenario. The *Type 2* mobility restriction outperforms the *Type 1* mobility restriction. This is because the former policy specially protects adults and elderlies. These age segments are more prone to die due to the disease, and thus reducing their mobility implies a significant decrease in deaths. For disobedience factors above 60%, the effect of the mobility restriction policies is very similar to the baseline scenario.
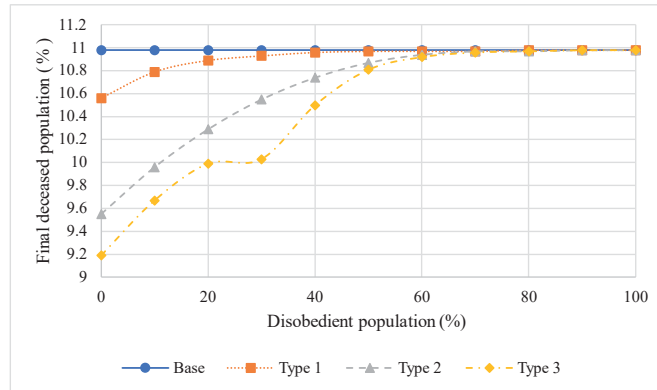
Figure 5. Effect of different of lockdown policies on the deceased compartment.

These case studies show the flexibility that the simulation environment brings to a variety of simulations, including a variety of parameters from age of the population up to quality of masks and degree of compliance with interventions. These modifications are simple to add when new research information is available. This framework includes Jupyter Notebooks to analyze the simulation logs and generate different charts to interpret the evolution of the epidemics. These additional visualization tools are also publicly available at the environment's GitHub repository.

6   CONCLUSIONS

We introduced a Cell-DEVS model to study the spread of pandemics using a SIRDS compartmental approach. The model allows us to quickly define prototypes related to the disease, and to visualize the simulation results for advanced analysis with simple configuration files. The use of a formal approach allows the modelers to focus on modeling aspects without worrying about the simulation low level complexities, which are handled by the tool. A base case SIRD scenario was simulated to describe its functionality. We also explored the effects of mobility reduction policies considering different levels of obedience. The effects on infection reduction due to restricted mobility were clear. As expected, there are variations in the overall infected population depending on the type of policy and the percentage of the population that follows the restrictions, which seems to be in agreement with the behavior of the spreading of a contagious disease under such control measures. The scenarios show the flexibility and potential of this platform to conduct simulation experiments of contagious disease spreading.

The proposed model library can represent social dynamics and supports rapid model changes, allowing policy makers to develop low-risk, evidence-informed, valid, and timely effective strategies to control the spreading of infectious diseases, like the current COVID-19 pandemic. Also, modelers can use this model as a basis to develop new algorithms to simulate different epidemics.

As future work, we intend to validate the proposed Cell-DEVS model against real-world data on COVID-19 spreading across a city. This will enable us to fine tune different parameters, like the appropriate population scale represented by each cell of the model for more accurate results. This will also help us to test the simulator performance, and to define a proper tradeoff between results precision and good performance.

REFERENCES

Anderson, R., and R. May 1992. *Infectious Diseases of Humans: Dynamics and Control*. OUP.
Aron, J., and I. Schwartz 1984. "Seasonality and Period-Doubling Bifurcations in an Epidemic Model". *Journal of Theoretical Biology* vol. 110 (4), pp. 665–679.

Belloli, L., D. Vicino, C. Ruiz-Martin, and G. Wainer 2019. "Building DEVS Models with the Cadmium Tool". In *Proceedings of the Winter Simulation Conference*, edited by N. Mustafee, M. Rabe, KH. G. Bae, C. Szabo, and S. Lazarova-molnar. National Harbor, MD, IEEE.

Bin, S., G. Sun, and C. Chen 2019. "Spread of Infectious Disease Modeling and Analysis of Different Factors on Spread of Infectious Disease Based on Cellular Automata". *International Journal of Environmental Research and Public Health* vol. 16 (23), pp. 4683.

Bjørnstad, O., K. Shea, M. Krzywinski, and N. Altman 2020. "The SEIRS Model for Infectious Disease Dynamics". *Nature Methods* vol. 17 (6), pp. 557–558.

Caccavo, D. 2020. "Chinese and Italian COVID-19 Outbreaks can be Correctly Described by a Modified SIRD Model." medRxiv doi: 10.1101/2020.03.19.20039388.

Calafiore, G., C. Novara, and C. Possieri 2020. "A Time-Varying SIRD Model for the COVID-19 Contagion in Italy". *Annual Reviews in Control* vol. 50, pp. 361.

Callejas, E., A. Inostrosa-Psijas, F. Moreno, M. Oyarzún, and R. Carvajal-Schiaffino 2020. "COVID-19 Transmission During a Tsunami Evacuation in a Lockdown City". In *39th International Conference of the Chilean Computer Science Society*, pp. 1–8. Coquimbo, Chile, IEEE.

Cárdenas, R., K. Henares, C. Ruiz-Martin, and G. Wainer 2020. "Cell-DEVS Models for the Spread of COVID-19". In *14th International Conference on Cellular Automata for Research and Industry,* pp. 239. Lodz, Poland, Springer Nature.

Chatterjee, S., A. Sarkar, S. Chatterjee, M. Karmakar, and R. Paul 2020. "Studying the Progress of COVID-19 Outbreak in India Using SIRD Model". *Indian Journal of Physics*, pp. 1–17.

Chitnis, N., J. Hyman, and J.Cushing 2008. "Determining Important Parameters in the Spread of Malaria Through the Sensitivity Analysis of a Mathematical Model". *Bullet. of Math. Biol.* vol. 70 (5), pp. 1272.

Cuevas, E. 2020. "An Agent-Based Model to Evaluate the COVID-19 Transmission Risks in Facilities". *Computers in Biology and Medicine* vol. 121, pp. 103827.

Dai, J., C. Zhai, J. Ai, J. Ma, J. Wang, and W. Sun 2021. "Modeling the Spread of Epidemics Based on Cellular Automata". *Processes* vol. 9 (1), pp. 55.

Danon, L., E. Brooks-Pollock, M. Bailey, and M. Keeling 2020. "A Spatial Model of COVID-19 transmission in England and Wales: Early Spread and Peak Timing". medRxiv doi: 10.1101/2020.02.12.20022566

Dietz, K. 1967. "Epidemics and Rumours: A Survey". *Journal of the Royal Statistical Society: Series A (General)* vol. 130 (4), pp. 505-528.

Du, H., L. Gardner, and E. Dong, 2020. "An Interactive Web-Based Dashboard to Track COVID-19 in Real Time". *Infectious Diseases* vol. 20 (5), pp. 533-534.

Fanelli, D., and F. Piazza 2020. "Analysis and Forecast of COVID-19 Spreading in China, Italy and France". *Chaos, Solitons & Fractals* vol. 134, pp. 109761.

Fernández, J., and C. Jones 2020. "Estimating and Simulating a SIRD Model of COVID-19 for Many Countries, States, and Cities". Technical Report No. 27128, National Bureau of Economic Research.

Fuentes, M., and M. Kuperman 1999. "Cellular Automata and Epidemiological Models with Spatial Dependence". *Physica A: Statistical Mechanics and its Applications* vol. 267, pp. 471-486.

Ghosh, S., and S. Bhattacharya 2020. "Computational Model on COVID-19 Pandemic Using Probabilistic Cellular Automata". arXiv preprint arXiv:2006.11270.

He, S., Y. Peng, and K. Sun 2020. "SEIR Modeling of the COVID-19 and its Dynamics". *Nonlinear Dynamics* vol. 101 (3), pp. 1667–1680.

Heesterbeek, H., R. Anderson, V. Andreasen, S. Bansal, D. De Angelis, C. Dye, et al. 2015. "Modeling Infectious Disease Dynamics in the Complex Landscape of Global Health". *Science* vol. 347 (6227).

Hoya White, S., A. Martín del Rey, and G. Rodríguez Sánchez 2007. "Modeling Epidemics Using Cellular Automata". *Applied Mathematics and Computation* vol. 186 (1), pp. 193–202.

Institute for Health Metrics and Evaluation. n.d. Current Social Distancing Assumed until Infections Minimized and Containment Implemented. Accessed April 17, 2020. https://covid19.healthdata.org/.

Johansen, A. 1996. "A Simple Model of Recurrent Epidemics". *J of Theor. Bio.* vol. 178 (1), pp. 45–51.

Karin, O., Y. Bar-On, T. Milo, I. Katzir, A. Mayo, et al. 2020. "Cyclic Exit Strategies from Lockdown to Suppress COVID-19 and Allow Economic Activity". medRxiv doi: 10.1101/2020.04.04.20053579.

Keeling M. and L. Danon 2009. "Mathematical Modelling of Infectious Diseases". *BMB* vol. 92(1).

Kermack, W. and A. McKendrick 1927. "A Contribution to the Mathematical Theory of Epidemics". In *Proceedings of the Royal Society of London*. Series A, pp. 700-721.

Khalil, H. and G. Wainer, 2020. "Cell-DEVS for Social Phenomena Modeling". *IEEE Transactions on Computational Social Systems* vol. 7 (3), pp. 725-740.

Kraemer, M., C. Yang, B. Gutierrez, C. Wu, B. Klein, D. Pigott, et al. 2020. "The Effect of Human Mobility and Control Measures on the COVID-19 Epidemic in China" *Science* vol. 368, pp. 493–497.

López, L., and X. Rodó, 2021. "A Modified SEIR Model to Predict the COVID-19 Outbreak in Spain and Italy: Simulating Control Scenarios and Multi-scale Epidemics". *Results in Physics* vol. 21, pp. 103746.

López, L., G. Burguerner, and L. Giovanini 2014. "Addressing Population Heterogeneity and Distribution in Epidemics Models using a Cellular Automata Approach". *BMC Research Notes* vol. 7 (1), pp. 1–11.

Medrek, M., and Z. Pastuszak 2021. "Numerical Simulation of the Novel Coronavirus Spreading". *Expert Systems with Applications* vol. 166, pp. 114109.

Muscatello, D. J, A. A. Chughtai, A. Heywood, L. M. Gardner, D. J. Heslop, and C. R. MacIntyre 2017. "Translation of Real-Time Infectious Disease Modeling into Routine Public Health Practice". *Emerging infectious diseases* vol. 23 (5), pp. e161720.

Ngwa, G. and W. Shu, 2000. "A Mathematical Model for Endemic Malaria with Variable Human and Mosquito Populations". *Mathematical and Computer Modelling* vol. 32 (7–8), pp. 747–763.

Nishiura, H., T. Kobayashi, T. Miyama, A. Suzuki, S. Jung, K. Hayashi, R. Kinoshita, et al. 2020. "Estimation of the Asymptomatic Ratio of Novel Coronavirus Infections (COVID-19)". *International Journal of Infectious Diseases* vol. 94, pp. 154.

Pacheco, C., and C. de Lacerda 2021. "Function Estimation and Regularization in the SIRD Model Applied to the COVID-19 Pandemics". *Inverse Problems in Science and Engineering*, pp. 1–16.

Rădulescu, A., C. Williams, and K. Cavanagh 2020. "Management Strategies in a SEIR-Type Model of COVID 19 Community Spread". *Scientific Report*s vol. 10 (1), pp. 1–16.

Small, M., and C. Tse 2005. "Small World and Scale Free Model of Transmission of SARS". *International Journal of Bifurcation and Chaos* vol. 15 (5), pp. 1745-1755.

Traoré, B., B. Sangaré, and S. Traoré 2017. "A Mathematical Model of Malaria Transmission with Structured Vector Population and Seasonality". *Journal of Applied Mathematics* vol. 2017.

Wainer, G. 2009. *Discrete-Event Modeling and Simulation: A Practitioner's Approach*. CRC Press.

Wolfram, S. 2002. *A New Kind of Science. vol. 5*. Champaign, IL: Wolfram media.

Wood, R., C. McWilliams, M. Thomas, C. Bourdeaux, and C. Vasilakis 2020. "COVID-19 Scenario Modelling for the Mitigation of Capacity-Dependent Deaths in Intensive Care". *Health Care Management Science* vol. 23 (3), pp. 315–324.

Zeigler, B., H. Praehofer, and T. Kim 2000. *Theory of Modeling and Simulation: Integrating Discrete Event and Continous Complex Dynamic Systems*. Academic Press.

Zhong, S., Q. Huang, and D. Song 2009. "Simulation of the Spread of Infectious Diseases in a Geographical Environment". *Science in China Series D: Earth Sciences* vol. 52 (4), pp. 550–561.

AUTHOR BIOGRAPHIES

ROMÁN CÁRDENAS is pursuing the Ph.D. in Electronic Systems Engineering in Cotutelle between Technical University of Madrid and Carleton University. His research interests include modeling and simulation with applications in the IoT domain. He can be reached at r.cardenas@upm.es.

ALONSO INOSTROSA-PSIJAS received the Ph.D. degree from Universidad de Santiago, Chile. He recently joined the School of Informatics Engineering at Universidad de Valparaiso, Chile. His research interests are discrete-event and parallel/distributed simulation. His e-mail is alonso.inostrosa@uv.cl.

GABRIEL WAINER received the Ph.D. degree from Université d'Aix-Marseille III. He is a Full Professor in Carleton University. His current research interests are related with modeling methodologies and tools, parallel/distributed simulation, and real-time systems. His e-mail is gwainer@sce.carleton.ca.